

A global study of the extended scalar singlet model

Ankit Beniwal^{1,2}

¹CoEPP and CSSM, Department of Physics, University of Adelaide, Australia

²Oskar Klein Centre, Department of Physics, Stockholm University, Sweden

Based on:

- A. Beniwal, M. Lewicki, M. White and A. G. Williams, *Gravitational waves and electroweak baryogenesis in a global study of the extended scalar singlet model*, in preparation for *JHEP*.

Preparing for Dark Matter Particle Discovery, Göteborg, Sweden

June 13, 2018



CoEPP
ARC Centre of Excellence for
Particle Physics at the Terascale



THE UNIVERSITY
of ADELAIDE



Oskar Klein
centre

- 1 Motivation
- 2 Model
- 3 Constraints
- 4 Likelihoods
- 5 Preliminary results
- 6 Conclusions

- Propose a viable dark matter (DM) candidate and explain the matter-antimatter asymmetry, i.e.,

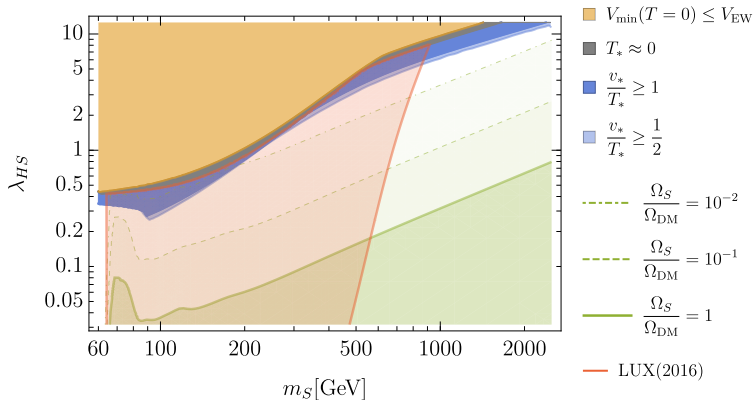
$$\eta \equiv \frac{n_B - n_{\bar{B}}}{n_\gamma} \approx 10^{-10}. \quad (1)$$

- From a homogeneous, baryon-symmetric Universe [1], we expect

$$\frac{n_B}{n_\gamma} = \frac{n_{\bar{B}}}{n_\gamma} \approx 10^{-20}.$$

- Require *dynamical* generation of asymmetry \rightarrow satisfy *Sakharov conditions* [2]
 - C and CP violation;
 - Baryon number (B) violation;
 - Departure from thermal equilibrium.
- Electroweak baryogenesis (EWBG): generation of asymmetry via a strong first-order electroweak phase transition (EWPT).
- All ingredients for EWBG are present in the Standard Model (SM).
- The SM alone is *not* enough to account for the asymmetry \rightarrow require new physics beyond the SM (BSM).
- Simplest BSM model: A \mathbb{Z}_2 symmetric scalar Higgs portal \rightarrow facilitate EWBG and provide a viable DM candidate.

- However, both puzzles *cannot* be solved simultaneously [3].



- Avoid DM constraints by proposing S as a new DM-SM mediator \rightarrow extended scalar singlet model + a fermionic DM candidate [4].
- Phase transition details mainly depend on S \rightarrow can hope to simultaneously solve both puzzles.

- Add a new real scalar singlet S and a Dirac fermion DM field ψ .
- Model Lagrangian is

$$\mathcal{L} = \mathcal{L}_{\text{SM}} + \mathcal{L}_S + \mathcal{L}_\psi + \mathcal{L}_{\text{portal}}, \quad (2)$$

where \mathcal{L}_{SM} is the SM Lagrangian,

$$\mathcal{L}_S = \frac{1}{2}(\partial_\mu S)(\partial^\mu S) + \frac{1}{2}\mu_S^2 S^2 + \frac{1}{3}\mu_3 S^3 - \frac{1}{4}\lambda_S S^4, \quad (3)$$

$$\mathcal{L}_\psi = \bar{\psi}(i\not{\partial} - \mu_\psi)\psi - g_S \bar{\psi}\psi S, \quad (4)$$

$$\mathcal{L}_{\text{portal}} = -\mu_{\Phi S}\Phi^\dagger\Phi S - \frac{1}{2}\lambda_{\Phi S}\Phi^\dagger\Phi S^2. \quad (5)$$

- Remove a linear term $\mu_1^3 S$ by a constant shift $S \rightarrow S + \sigma$.
- When $\mu_3 = g_S = \mu_{\Phi S} = 0 \rightarrow$ scalar Higgs portal [5].

- Tree-level scalar potential is

$$V_{\text{tree}} = -\mu_{\Phi}^2 \Phi^\dagger \Phi + \lambda_{\Phi} (\Phi^\dagger \Phi)^2 + V_S + V_{\text{portal}}, \quad (6)$$

where

$$\Phi = \begin{pmatrix} G^+ \\ \frac{1}{\sqrt{2}}(\phi + iG^0) \end{pmatrix} \quad (7)$$

is the SM Higgs doublet.

- Both ϕ and S can develop non-trivial VEVs. At $T = 0$, they are

$$\langle 0|\phi|0\rangle|_{T=0} = v_0, \quad \langle 0|S|0\rangle|_{T=0} = s_0. \quad (8)$$

- After electroweak symmetry breaking (EWSB), we get

$$\Phi = \frac{1}{\sqrt{2}} \begin{pmatrix} 0 \\ v_0 + \varphi \end{pmatrix}, \quad S = s_0 + s. \quad (9)$$

- $\mathcal{L}_{\text{portal}} \rightarrow$ mixing between φ and s , i.e., \mathcal{M}^2 is non-diagonal.
- Define mass eigenstates (h, H) by

$$\begin{pmatrix} h \\ H \end{pmatrix} = \begin{pmatrix} \cos \alpha & -\sin \alpha \\ \sin \alpha & \cos \alpha \end{pmatrix} \begin{pmatrix} \varphi \\ s \end{pmatrix}, \quad (10)$$

where α is the mixing angle.

- Tree-level potential must be bounded from below, i.e.,

$$\lambda_{\Phi} > 0, \quad \lambda_S > 0, \quad \lambda_{\Phi S} > -2\sqrt{\lambda_{\Phi}\lambda_S}. \quad (11)$$

- The fermion DM Lagrangian after EWSB is

$$\mathcal{L}_{\psi} = \bar{\psi}(i\not{\partial} - m_{\psi})\psi - g_S\bar{\psi}\psi s, \quad (12)$$

where

$$m_{\psi} = \mu_{\psi} + g_S s_0. \quad (13)$$

- With the Higgs boson discovery at the LHC, we set

$$m_h = 125.13 \text{ GeV}, \quad v_0 = 246.22 \text{ GeV}. \quad (14)$$

- The model contains 7 free parameters, namely

$$m_H, \quad s_0, \quad \mu_3, \quad \lambda_S, \quad \alpha, \quad m_\psi, \quad g_S. \quad (15)$$

- Remaining parameters are given by

$$\lambda_\Phi = \frac{1}{2v_0^2} (m_h^2 \cos^2 \alpha + m_H^2 \sin^2 \alpha), \quad (16)$$

$$\mu_{\Phi S} = -\frac{2s_0}{v_0^2} (m_h^2 \sin^2 \alpha + m_H^2 \cos^2 \alpha + \mu_3 s_0 - 2\lambda_S s_0^2), \quad (17)$$

$$\lambda_{\Phi S} = \frac{1}{v_0 s_0} [(m_H^2 - m_h^2) \sin \alpha \cos \alpha - \mu_{\Phi S} v_0], \quad (18)$$

$$\mu_\Phi^2 = \lambda_\Phi v_0^2 + \mu_{\Phi S} s_0 + \frac{1}{2} \lambda_{\Phi S} s_0^2, \quad (19)$$

$$\mu_S^2 = -\mu_3 s_0 + \lambda_S s_0^2 + \frac{\mu_{\Phi S} v_0^2}{2s_0} + \frac{1}{2} \lambda_{\Phi S} v_0^2. \quad (20)$$

- Implement the model in micrOMEGAs_v4.3.5 [6] via LanHEP_v3.2.0 [7].

- ① **DM relic density:** require $\Omega_\psi h^2 \leq \Omega_{\text{DM}} h^2 = 0.1188$ from *Planck* [8].
- ② **Direct detection:** require $\sigma_{\text{SI}}^{\text{eff}} \leq \sigma_{\text{PandaX-II}}$ where $\sigma_{\text{PandaX-II}} = 90\%$ C.L. upper limit from PandaX-II [9] and

$$\sigma_{\text{SI}}^{\text{eff}} = \frac{\mu_{\psi\mathcal{N}}^2}{\pi} \left(\frac{g_S \sin \alpha \cos \alpha}{v_0} \right)^2 \left(\frac{1}{m_h^2} - \frac{1}{m_H^2} \right)^2 m_{\mathcal{N}}^2 f_{\mathcal{N}}^2 \left(\frac{\Omega_\psi}{\Omega_{\text{DM}}} \right).$$

- ③ **EWBG:** require $v_c/T_c \geq 0.6$ where $v_c = \text{Higgs VEV at the critical temperature } T_c$.
- ④ **Electroweak precision observables (EWPO):** require

$$\Delta\mathcal{O} \equiv \mathcal{O} - \mathcal{O}_{\text{SM}} = (1 - \cos^2 \alpha) \left[\mathcal{O}_{\text{SM}}(m_H) - \mathcal{O}_{\text{SM}}(m_h) \right], \quad (21)$$

where $\mathcal{O} \in (S, T, U)$ to agree with the global electroweak fit results [10].

- ⑤ **Direct Higgs searches:** searches for a SM-like Higgs boson at the LEP, Tevatron and the LHC [11].
- ⑥ **Higgs signal strength measurements:** Higgs signal strength and mass measurements performed at the LHC [12]. The Higgs signal strengths are

$$\mu_h = \frac{\Gamma_h^{\text{SM}} \cos^4 \alpha}{\Gamma_h^{\text{SM}} \cos^2 \alpha + \Gamma_{h \rightarrow \bar{\psi}\psi} + \Gamma_{h \rightarrow HH}}, \quad \mu_H = \frac{\Gamma_H^{\text{SM}} \sin^4 \alpha}{\Gamma_H^{\text{SM}} \sin^2 \alpha + \Gamma_{H \rightarrow \bar{\psi}\psi} + \Gamma_{H \rightarrow hh}}.$$

- Adopt a frequentist approach and perform 7D scans using Diver_v1.0.4 [13].*
- The combined log-likelihood function is

$$\ln \mathcal{L}_{\text{total}}(\boldsymbol{\theta}|\mathcal{D}) = \ln \mathcal{L}_{\Omega h^2}(\boldsymbol{\theta}|\mathcal{D}) + \ln \mathcal{L}_{\text{PandaX-II}}(\boldsymbol{\theta}|\mathcal{D}) + \ln \mathcal{L}_{\nu_c/T_c}(\boldsymbol{\theta}|\mathcal{D}) \\ + \ln \mathcal{L}_{\text{EWPO}}(\boldsymbol{\theta}|\mathcal{D}) + \ln \mathcal{L}_{\text{HB}}(\boldsymbol{\theta}|\mathcal{D}) + \ln \mathcal{L}_{\text{HS}}(\boldsymbol{\theta}|\mathcal{D}), \quad (22)$$

where $\boldsymbol{\theta} \equiv (m_H, s_0, \mu_3, \lambda_S, \alpha, m_\psi, g_S)$ and $\mathcal{D} =$ experimental data.

Likelihoods	Description	Functional form/Source
$\ln \mathcal{L}_{\Omega h^2}(\boldsymbol{\theta} \mathcal{D})$	relic density likelihood	1-sided Gaussian (upper)
$\ln \mathcal{L}_{\text{PandaX-II}}(\boldsymbol{\theta} \mathcal{D})$	direct detection likelihood	1-sided Gaussian (upper)
$\ln \mathcal{L}_{\nu_c/T_c}(\boldsymbol{\theta} \mathcal{D})$	EWBG likelihood	1-sided Gaussian (lower)
$\ln \mathcal{L}_{\text{EWPO}}(\boldsymbol{\theta} \mathcal{D})$	EWPO likelihood	3D Gaussian (correlated)
$\ln \mathcal{L}_{\text{HB}}(\boldsymbol{\theta} \mathcal{D})$	Direct Higgs searches likelihood	HiggsBounds_v4.3.1
$\ln \mathcal{L}_{\text{HS}}(\boldsymbol{\theta} \mathcal{D})$	Higgs signal strength likelihood	HiggsSignals_v1.4.0

*<http://diver.hepforge.org>

- Our choice for the free parameter ranges and priors are

Parameter	Minimum	Maximum	Prior type
m_H	10 GeV	10 TeV	log
s_0	-1 TeV	1 TeV	flat
μ_3	-1 TeV	1 TeV	flat
λ_S	10^{-3}	10	log
α	0	$\pi/2$	flat
m_ψ	10 GeV	10 TeV	log
g_S	10^{-3}	10	log

- Present results in the form of 1D and 2D profile likelihoods where

$$\mathcal{L}_p(\theta_i|\mathcal{D}) = \max_{\{\theta_j|j\neq i\}} \mathcal{L}(\boldsymbol{\theta}|\mathcal{D}), \quad \mathcal{L}_p(\theta_i, \theta_j|\mathcal{D}) = \max_{\{\theta_k|k\neq i, j\}} \mathcal{L}(\boldsymbol{\theta}|\mathcal{D}). \quad (23)$$

- Construct 1σ and 2σ C.L. contours around the best-fit point $\hat{\boldsymbol{\theta}}$ using Wilks' theorem with

$$\Lambda(\theta_i) = \frac{\mathcal{L}_p(\theta_i|\mathcal{D})}{\mathcal{L}(\hat{\boldsymbol{\theta}}|\mathcal{D})}, \quad \Lambda(\theta_i, \theta_j) = \frac{\mathcal{L}_p(\theta_i, \theta_j|\mathcal{D})}{\mathcal{L}(\hat{\boldsymbol{\theta}}|\mathcal{D})}. \quad (24)$$

Find regions in the model parameter space where a successful EWBG is viable using

$$\ln \mathcal{L}_{\text{total}}(\boldsymbol{\theta}|\mathcal{D}) = \ln \mathcal{L}_{v_c/T_c}(\boldsymbol{\theta}|\mathcal{D}). \quad (25)$$

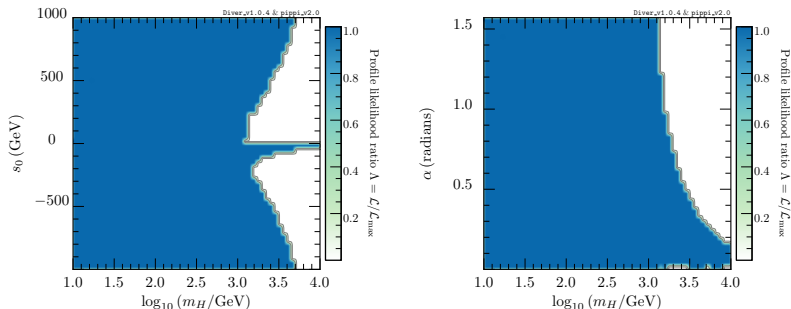
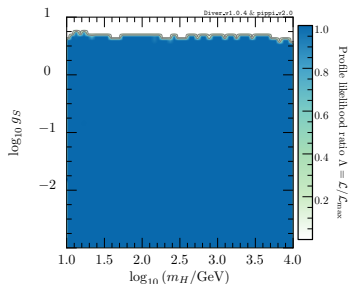
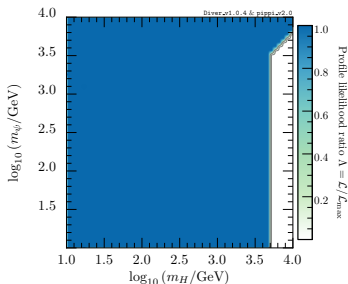
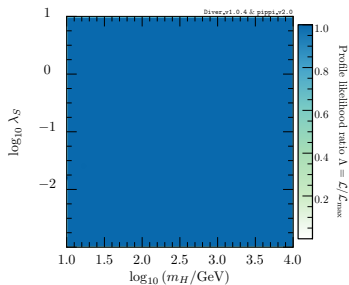
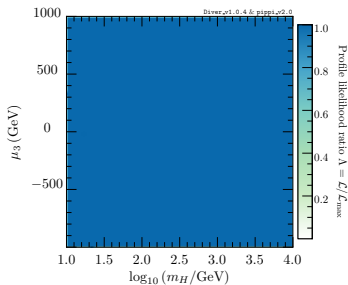


Fig. 1: 2D profile likelihood in the (m_H, s_0) and (m_H, α) plane.



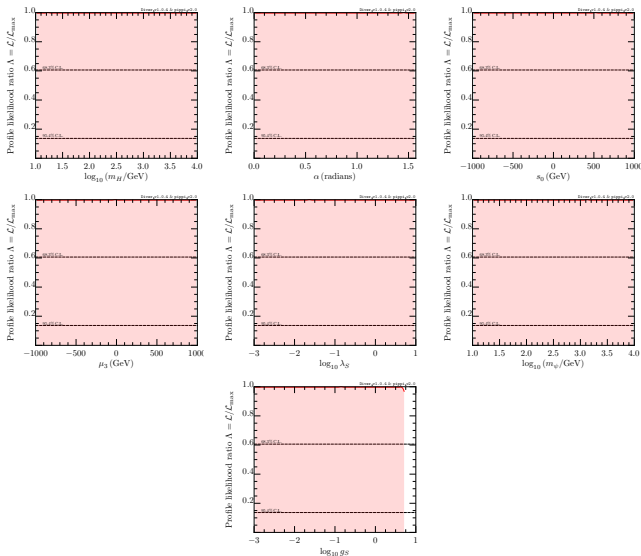


Fig. 2: 1D profile likelihood for the free model parameters.

Find regions that are compatible with all constraints using

$$\ln \mathcal{L}_{\text{total}}(\boldsymbol{\theta}|\mathcal{D}) = \ln \mathcal{L}_{\Omega h^2}(\boldsymbol{\theta}|\mathcal{D}) + \ln \mathcal{L}_{\text{PandaX-II}}(\boldsymbol{\theta}|\mathcal{D}) + \ln \mathcal{L}_{\nu_c/T_c}(\boldsymbol{\theta}|\mathcal{D}) \\ + \ln \mathcal{L}_{\text{EWPO}}(\boldsymbol{\theta}|\mathcal{D}) + \ln \mathcal{L}_{\text{HB}}(\boldsymbol{\theta}|\mathcal{D}) + \ln \mathcal{L}_{\text{HS}}(\boldsymbol{\theta}|\mathcal{D}). \quad (26)$$

Best-fit point is found at

m_H (GeV)	s_0 (GeV)	μ_3 (GeV)	λ_S	α	m_ψ (GeV)	g_S
125.127	156.545	55.379	0.227	3.774×10^{-2}	300.670	1.107

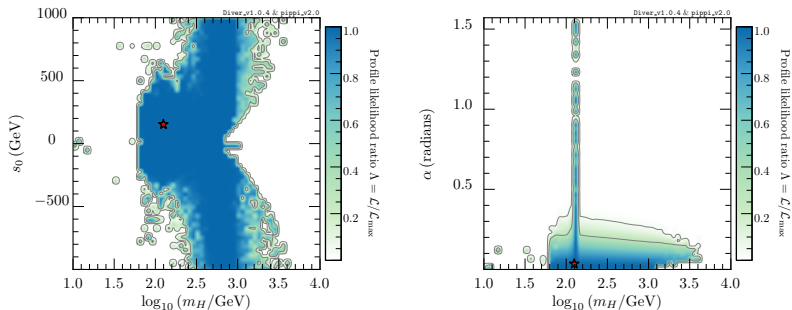
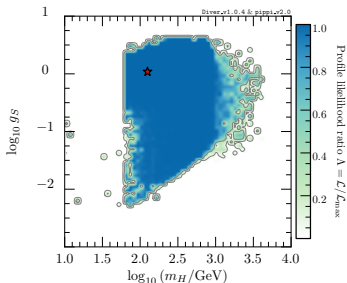
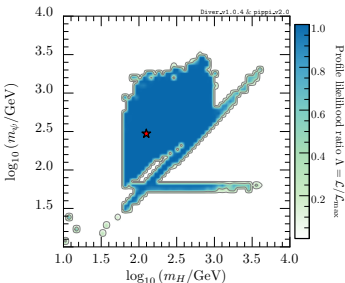
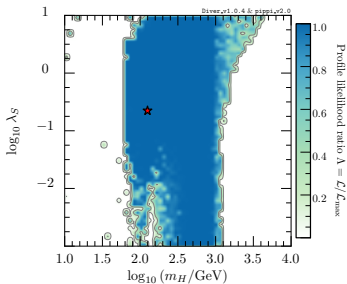
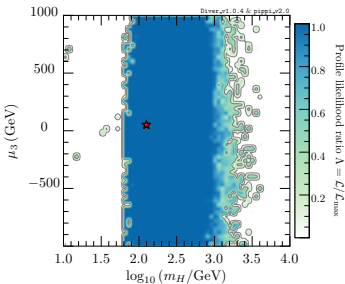


Fig. 3: 2D profile likelihood in the (m_H, s_0) and (m_H, α) plane.

Preliminary results

Global fit



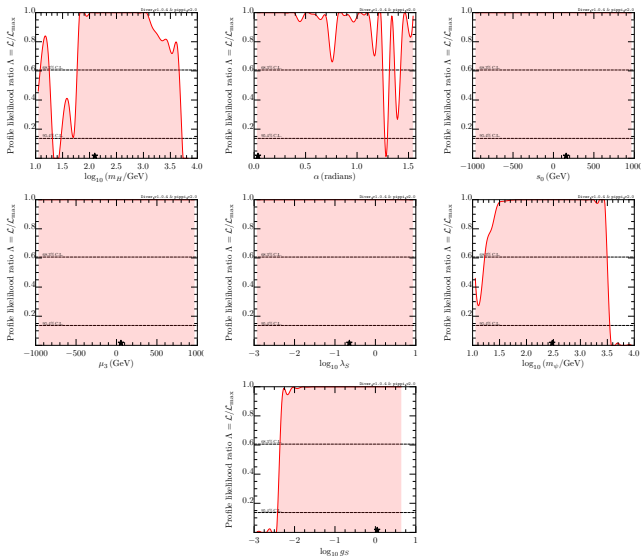


Fig. 4: 1D profile likelihood for the free model parameters.

A strong first-order phase transition \implies a strong gravitational wave (GW) signal \rightarrow prospects for detection at future GW experiments.

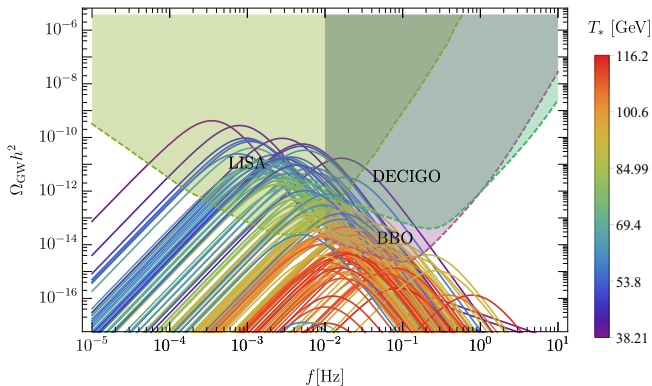


Fig. 5: GW spectra of viable points and their dependence on the transition temperature T_* . Projected sensitivity bands of future GW experiments such as LISA, DECIGO and BBO are also shown.

A strong first-order phase transition \implies a strong gravitational wave (GW) signal \rightarrow detection prospects at future GW experiments.

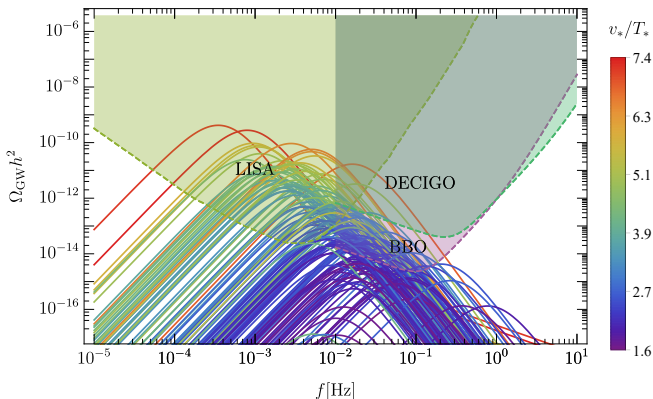


Fig. 6: Same as the previous figure except for the dependence on the dimensionless parameter v_*/T_* .

- Performed a comprehensive and up-to-date study of the extended scalar singlet model with a fermionic DM candidate.
- Found regions that can facilitate EWBG. In particular, one requires $g_S \lesssim 5.62$.
- Found regions that are compatible with all constraints \rightarrow upper limit on m_H , m_ψ and g_S .
- GW spectra of viable points are often within reach of future GW experiments such as LISA, DECIGO and BBO.

Future plans:

- ① Run a combined 7D scan using the latest XENON1T (2018) result.
 - ② Run a combined 7D scan with $f_{\text{rel}} \equiv \Omega_\psi / \Omega_{\text{DM}} = 1$.
-

Backup slides

- A hot, radiation-dominated early Universe with zero baryon charge and full EW symmetry, i.e., $\langle \phi \rangle = 0$.
- When $T \lesssim 100$ GeV (EW scale), ϕ develops a VEV \rightarrow EW symmetry is broken.
- Baryon asymmetry is generated when the Universe transitions from $\langle \phi \rangle = 0$ to $\langle \phi \rangle \neq 0$.

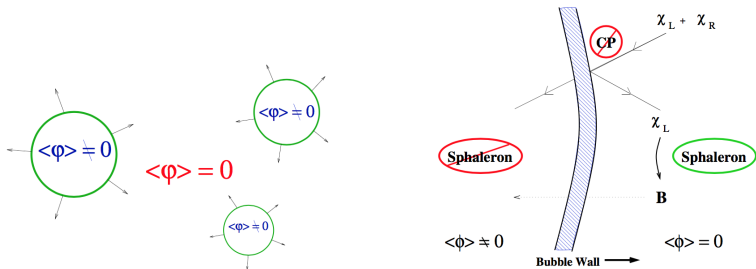


Fig. 7: *Left panel:* Expanding bubbles of the broken phase around the plasma in the symmetric phase. *Right panel:* Baryon production in front of the bubble walls. Figure from Ref. [14].

- Key ingredient is the effective potential

$$V_{\text{eff}}(\phi, T) = V_{\text{tree}}(\phi) + V_{1\text{-loop}}(\phi) + V_T(\phi, T).$$

- At high T , $V_T(\phi, T)$ restores the EW symmetry, i.e., $\langle \phi \rangle = 0$.
- When $T = T_c$ (critical temperature), $\langle \phi \rangle = 0$ and $\langle \phi \rangle \neq 0$ minima are *degenerate*.
- If the two minimas are separated by a potential barrier \rightarrow a first-order phase transition occurs, i.e.,

$$\frac{v_c}{T_c} \gtrsim 1,$$

where $v_c = \text{Higgs VEV at } T = T_c$.

- In the SM, $v_c/T_c \gtrsim 1$ only if $m_h \lesssim 70 \text{ GeV}$ [15] \rightarrow a smooth cross-over.
- New scalar-Higgs couplings can give $v_c/T_c \gtrsim 1$ for $m_h = 125 \text{ GeV}$.

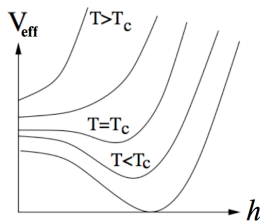
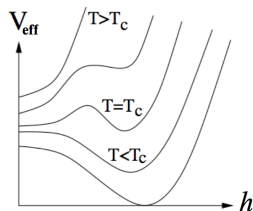


Fig. 8: Evolution of $V_{\text{eff}}(h, T)$ with T for a first- (top panel) and second- (bottom panel) order phase transition. Figure from Ref. [16].

3 main sources of GWs from a strong first-order PT:

- ① Collision of the bubble walls [17];
- ② Sound waves generated after the phase transition [18];
- ③ Magneto-hydrodynamical (MHD) turbulence in the plasma [19].

These depend on the following parameters:

- ① Ratio of the released latent heat to the plasma background [20]

$$\alpha = \frac{1}{\rho_R} \left[-(V_{EW} - V_f) + T \left(\frac{dV_{EW}}{dT} - \frac{dV_f}{dT} \right) \right] \Big|_{T=T_*}, \quad (27)$$

where V_f = value of the potential in the unstable vacuum.

- ② Characteristic rate of bubble nucleation

$$\frac{\beta}{H} = \left[T \frac{d}{dT} \left(\frac{S_3(T)}{T} \right) \right] \Big|_{T=T_*}, \quad (28)$$

where $S_3 = \mathcal{O}(3)$ symmetric action and H = Hubble rate.

- ③ Bubble wall velocity v_b .

The combined GW spectra is

$$\Omega_{\text{GW}} h^2(f) = \Omega h_{\text{col}}^2(f) + \Omega h_{\text{sw}}^2(f) + \Omega h_{\text{turb}}^2(f). \quad (29)$$

Bubble collisions: Peak frequency is [17]

$$f_{\text{col}} = 16.5 \times 10^{-6} \frac{0.62}{v_b^2 - 0.1v_b + 1.8} \frac{\beta}{H} \frac{T_*}{100} \left(\frac{g_*}{100} \right)^{1/6} \text{ Hz.}$$

The energy density is

$$\Omega_{\text{col}}^2(f) = 1.67 \times 10^{-5} \left(\frac{\beta}{H} \right)^{-2} \frac{0.11v_b^3}{0.42 + v_b^2} \left(\frac{\kappa\alpha}{1 + \alpha} \right)^2 \left(\frac{g_*}{100} \right)^{-1/3} \frac{3.8 (f/f_{\text{col}})^{2.8}}{1 + 2.8 (f/f_{\text{col}})^{3.8}},$$

where the efficiency factor κ and the bubble wall velocity v_b is

$$\kappa = \frac{\alpha_\infty}{\alpha} \left(\frac{\alpha_\infty}{0.73 + 0.083\sqrt{\alpha_\infty} + \alpha_\infty} \right),$$

$$v_b = \frac{1/\sqrt{3} + \sqrt{\alpha^2 + 2\alpha/3}}{1 + \alpha}.$$

For a very strong phase transition, the energy deposited into the fluid saturates at

$$\alpha_\infty = 0.49 \times 10^{-3} \left(\frac{v_*}{T_*} \right)^2.$$

Sound waves created in the plasma: Peak frequency is [18]

$$f_{\text{sw}} = 1.9 \times 10^{-5} \frac{\beta}{H} \frac{1}{v_b} \frac{T_*}{100} \left(\frac{g_*}{100} \right)^{1/6} \text{ Hz.}$$

The energy density is

$$\Omega h_{\text{sw}}^2(f) = 2.65 \times 10^{-6} \left(\frac{\beta}{H} \right)^{-1} \left(\frac{\kappa\alpha}{1+\alpha} \right)^2 \left(\frac{g_*}{100} \right)^{-1/3} v_b \left(\frac{f}{f_{\text{sw}}} \right)^3 \left(\frac{7}{4+3(f/f_{\text{sw}})^2} \right)^{7/2}.$$

MHD turbulence in the plasma: Peak frequency is [20]

$$f_{\text{turb}} = 2.7 \times 10^{-5} \frac{\beta}{H} \frac{1}{v_b} \frac{T_*}{100} \left(\frac{g_*}{100} \right)^{1/6} \text{ Hz.}$$

The energy density is

$$\Omega h_{\text{turb}}^2(f) = 3.35 \times 10^{-4} \left(\frac{\beta}{H} \right)^{-1} \left(\frac{\epsilon\kappa\alpha}{1+\alpha} \right)^{3/2} \left(\frac{g_*}{100} \right)^{-1/3} v_b \frac{(f/f_{\text{turb}})^3 (1+f/f_{\text{turb}})^{-11/3}}{[1+8\pi f a_0/(a_* H_*)]},$$

where $a_*(H_*) = \text{scale (Hubble) factor at } T = T_*$ and $\epsilon \approx 0.05 = \text{efficiency factor}$.

- [1] E. W. Kolb and M. S. Turner, *The Early Universe*, *Front. Phys.* **69** (1990) 1–547.
- [2] A. D. Sakharov, *Violation of CP Invariance, C Asymmetry, and Baryon Asymmetry of the Universe*, *Pisma Zh. Eksp. Teor. Fiz.* **5** (1967) 32–35.
- [3] A. Beniwal, M. Lewicki, J. D. Wells, M. White and A. G. Williams, *Gravitational wave, collider and dark matter signals from a scalar singlet electroweak baryogenesis*, *JHEP* **08** (2017) 108, [[1702.06124](#)].
- [4] S. Baek, P. Ko and W.-I. Park, *Search for the Higgs portal to a singlet fermionic dark matter at the LHC*, *JHEP* **02** (2012) 047, [[1112.1847](#)].
- [5] GAMBIT collaboration, P. Athron et al., *Status of the scalar singlet dark matter model*, *Eur. Phys. J. C* **77** (2017) 568, [[1705.07931](#)].
- [6] G. Blanger, F. Boudjema, A. Pukhov and A. Semenov, *micrOMEGAs4.1: two dark matter candidates*, *Comput. Phys. Commun.* **192** (2015) 322–329, [[1407.6129](#)].
- [7] A. Semenov, *LanHEP - A package for automatic generation of Feynman rules from the Lagrangian. Version 3.2*, *Comput. Phys. Commun.* **201** (2016) 167–170, [[1412.5016](#)].
- [8] PLANCK collaboration, P. A. R. Ade et al., *Planck 2015 results. XIII. Cosmological parameters*, *Astron. Astrophys.* **594** (2016) A13, [[1502.01589](#)].
- [9] PANDA-X-II collaboration, X. Cui et al., *Dark Matter Results From 54-Ton-Day Exposure of PandaX-II Experiment*, *Phys. Rev. Lett.* **119** (2017) 181302, [[1708.06917](#)].
- [10] J. Haller, A. Hoecker, R. Kogler, K. Mnig, T. Peiffer and J. Stelzer, *Update of the global electroweak fit and constraints on two-Higgs-doublet models*, [1803.01853](#).
- [11] P. Bechtle, O. Brein, S. Heinemeyer, O. Stal, T. Stefaniak, G. Weiglein et al., *HiggsBounds – 4: Improved Tests of Extended Higgs Sectors against Exclusion Bounds from LEP, the Tevatron and the LHC*, *Eur. Phys. J. C* **74** (2014) 2693, [[1311.0055](#)].

- [12] P. Bechtle, S. Heinemeyer, O. Stal, T. Stefaniak and G. Weiglein, *HiggsSignals: Confronting arbitrary Higgs sectors with measurements at the Tevatron and the LHC*, *Eur. Phys. J.* **C74** (2014) 2711, [1305.1933].
- [13] GAMBIT SCANNER WORKGROUP collaboration, G. Martinez, D., J. McKay, B. Farmer, P. Scott, E. Roeber et al., *Comparison of statistical sampling methods with ScannerBit, the GAMBIT scanning module*, 1705.07959.
- [14] D. E. Morrissey and M. J. Ramsey-Musolf, *Electroweak baryogenesis*, *New J. Phys.* **14** (2012) 125003, [1206.2942].
- [15] A. Bochkarev and M. Shaposhnikov, *Electroweak production of baryon asymmetry and upper bounds on the higgs and top masses*, *Modern Physics Letters A* **02** (1987) 417–427, [<http://www.worldscientific.com/doi/pdf/10.1142/S0217732387000537>].
- [16] J. M. Cline, *Baryogenesis*, in *Les Houches Summer School - Session 86: Particle Physics and Cosmology: The Fabric of Spacetime Les Houches, France, July 31-August 25, 2006*, 2006. [hep-ph/0609145](http://arxiv.org/abs/hep-ph/0609145).
- [17] S. J. Huber and T. Konstandin, *Gravitational Wave Production by Collisions: More Bubbles*, *JCAP* **0809** (2008) 022, [0806.1828].
- [18] M. Hindmarsh, S. J. Huber, K. Rummukainen and D. J. Weir, *Gravitational waves from the sound of a first order phase transition*, *Phys. Rev. Lett.* **112** (2014) 041301, [1304.2433].
- [19] C. Caprini, R. Durrer and G. Servant, *The stochastic gravitational wave background from turbulence and magnetic fields generated by a first-order phase transition*, *JCAP* **0912** (2009) 024, [0909.0622].
- [20] C. Caprini et al., *Science with the space-based interferometer eLISA. II: Gravitational waves from cosmological phase transitions*, *JCAP* **1604** (2016) 001, [1512.06239].